

Two Approaches to Kinetic Analysis Applied to the Prediction of Antioxidant Activity

A. L. Pomerantsev and O. Ye. Rodionova

Semenov Institute of Chemical Physics, Russian Academy of Sciences, Moscow, 117977 Russia

e-mail: forecast@chph.ras.ru

Received December 28, 2004

Abstract—Differential scanning calorimetry (DSC) followed by mathematical data processing can be used instead of the conventional method of long term thermal aging in predicting the activity of antioxidants in polyolefins. In this method, a regression relationship is established between the oxidation initial temperatures measured by DSC (X data) and the oxidation induction period values determined by thermal aging (Y data). Two approaches, called hard and soft, are employed in the construction of models. In the first case, nonlinear regression analysis is used in combination with successive Bayesian estimation. The second approach combines partial least squares regression and simple interval calculation. Use of a common data set makes it possible to compare these approaches and to draw inferences as to the cases in which one or the other is preferable.

DOI: 10.1134/S0023158406040094

Data analysis and mechanistic studies for complex chemical processes are the most important areas of chemical kinetics. Estimating kinetic parameters from experimental data or, in other words, solving the inverse problem of chemical kinetics was formed as an individual area in the 1970s–1980s. Mathematicians [1, 2], as well as kineticists [3, 4], have taken part in the development of this area. Two main, fundamentally different approaches to the problem of kinetic data analysis can be distinguished. In the so-called soft approach [5–13], experimental data are described in terms of a linear multivariate model valid in a limited range of conditions. In this case, it is not necessary to know the mechanism of the process. However, this approach does not always provide the desired accuracy. The other approach uses so-called hard physicochemical modeling [4, 14], which is based on fundamental kinetic principles and allows parameters to be estimated with a high degree of accuracy. However this method is applicable only when a model of the process is known a priori. Both approaches have strong and weak points, and both have advocates and opponents. Traditionally, Russian researchers develop the hard approach [15], while Western researchers prefer soft methods [16].

The problem of data interpretation, model construction, and prediction of unknown values (called calibration for brevity) is among the oldest but still challenging scientific problems. Since Gauss (1794), this problem has been attacked using regression analysis. The basic principle of this method is minimizing the deviation of the model from experimental data (least-squares method) [17]. The development of this approach, including principal component analysis (1901) [18], the maximum likelihood method (1912) [19], ridge

regression (1963) [20], and projection on latent structures (PLS, 1975) [21], has made it applicable to complex, ill-posed problems. However, all of these methods provide predictions as point estimates, whereas interval estimates taking into account the uncertainty of prediction are often required in practice. Constructing confidence intervals using conventional statistical methods is impossible because of the complexity of the problem [22], and employing simulation methods is impossible because of the long computational time required [23].

In 1962, Kantorovich [24] suggested another approach to the problem of linear calibration, which is to replace the objection function by a set of inequalities solvable by linear programming methods. In this case, the result of prediction appears immediately as an interval estimate. For this reason, this method was named simple interval calculation (SIC). Previously, this idea did not gain wide acceptance and was not developed because of inadequate computer performance. In the 1970s–1990s, this approach was taken in a series of interesting applied studies [25–32] but was not developed into a standard method. The results of those investigations were summed up in a monograph [33], where the main problem solved by the authors of the above-mentioned works is considered in detail. This problem includes the interval estimation of the model parameters and the immersion of the admitted region of these parameters into a hypercube, parallelepiped, ellipsoid, etc.

This problem formulation seems to be unprofitable and not very promising. This view is proved by the fact that no new works using this approach have been carried out in the last decade. At the same time, we believe that Kantorovich's idea can provide interesting results when applied to the interval prediction of response. In

this case, it is possible to solve two equally important practical problems. The first is to establish the uncertainty interval for the required response prediction [34] (that is, to estimate the accuracy of the constructed model for each particular sample). The second is to construct an object status classification [35] (that is, to determine the specific features of each sample, which are defined by the relationships between this sample and the model, and between this sample and other samples). Well-known concepts of such classification are the outlier (which is a sample standing far out from the general regularity) and the extreme sample (which is a sample lying in the model fringe region and having a profound influence on model construction). In spite of the wide use of these concepts in various investigations [36–44], there are no universally recognized definitions and detection methods for such objects. The SIC approach can fill this gap.

The theoretical aspects of SIC were reported in [35, 45, 46], and the practical results obtained by this method were discussed in [47–49]. The main assumption underlying the SIC method is the finiteness of the measurement error. This approach to the interpretation of experimental data requires some substantiation. Error normality is a standard assumption in data analysis. This principle has been repeatedly criticized from various standpoints [49–51]. It is interesting that researchers do not relate the fact of error infiniteness to the principle of normality. The direct question of how frequently the researcher has had to process data containing values lying beyond four standard deviations (4σ) is usually followed by the answer that such values have been resolutely screened out at the preprocessing stage. At the same time, researchers often deal with data sets containing over 10^6 data [52], out of which some 20–30 objects will certainly fall beyond the 4σ limit. According to the authors of [43], “indeed, in real case studies, the chemist is often able to select, to some degree, the samples, and this will lead to more uniform distribution than normal distribution.” A detailed analysis of this problem is presented in [45].

In the present article, the hard and soft approaches to kinetic data analysis are compared by applying them to the evaluation of the efficiency of antioxidants in polyolefins. Note that we will not predict the activity of a new compound by familiar QSAR methods [53, 54] using known molecular descriptors. In the example considered here, we test the quality of existing compounds that are expected, with good reason, to be antioxidants. For this purpose, kinetic data obtained by differential scanning calorimetry (DSC) are employed. This approach allows the testing time to be significantly shortened by doing away with the traditional expensive procedure in which samples are held in a furnace for 1–3 months. DSC kinetic data are oxidation initial temperatures for various heating rates. They form an X data set, which is calibrated against a Y set consisting of the oxidation induction period values obtained by a conventional method. Two $Y = F(X)$ calibration models

were employed, namely, a soft linear dependence and a hard nonlinear model in which contemporary conceptions of the mechanism of polyolefin oxidation are taken into account [55]. In the construction of the first model, we used a multivariate linear regression [5] in which prediction intervals are obtained by SIC. In the hard model, nonlinear regression analysis [56] was employed and traditional confidence intervals were constructed using the successive Bayesian estimation approach [57, 58]. Thus, the soft and hard modeling approaches were applied to one set of experimental data. This has made it possible to compare the results and to see which approach is preferable in a given case.

EVALUATION OF ANTIOXIDANT ACTIVITY

The determination of antioxidant efficiency in polyolefins is a long and expensive process. In conventional antioxidant testing procedures, samples are held at a constant temperature for a long time. However, an alternative approach enabling the researcher to quickly predict the antioxidant activity can be applied. The idea of using DSC for this purpose was suggested and analyzed earlier [48, 59, 60]. Both hard [58] and soft [48] approaches were employed in modeling in those works. However the data used fell within a limited range. In the present article, a rather representative antioxidant sample set is investigated. This makes it possible to solve two important problems. The first problem is that of the applicability of the alternative approach. The second is to compare the hard and soft modeling approaches using the same set of experimental data.

Antioxidants are special admixtures slowing down the thermal oxidative aging of polymers. They protect a material against oxidation during processing as well as at the end-use application. Interacting with free radicals, the antioxidant terminates chains and is thus exhausted. It completely suppresses oxidation as long as its concentration exceeds some critical value. That is why the main measure of antioxidant efficiency is the oxidation induction period (OIP), which is the time period within which the antioxidant concentration is sufficiently high. The greater OIP, the higher the efficiency of the antioxidant (at a fixed temperature). The induction period is conventionally determined by the long-term thermal aging (LTHA) of samples at 120–140°C. The exposure time depends on antioxidant quality and varies between 1 day for a poor antioxidant and 100 days for a good antioxidant. Within this period, a researcher examines the samples in search of obvious signs of degradation, such as cracking, yellowing, etc. It is clear that this approach is unreliable, very time-consuming, and expensive.

Alternative to this approach is the method using DSC measurements followed by mathematical data processing. In DSC, the measured signal is the heat flux from a sample heated at a constant rate. If a chemical reaction with nonzero heat takes place in the sample,

there will be a DSC signal proportional to the reaction rate. Regarding the problem examined, this means that as long as the antioxidant concentration is sufficient for the suppression of free-radical oxidation, the DSC signal is constant, but, starting at some temperature, it begins to grow rapidly. This temperature is called the oxidation initial temperature (OIT). Different OIT values can be obtained in runs carried out at different heating rates (y).

EXPERIMENTAL

Twenty-five antioxidant samples (AO-1 to AO-25) were tested. Some of them (for example, AO-1, AO-2, and AO-3) are standard commercial admixtures. The other samples are new compounds expected to be effective. All samples were added to polypropylene (PP) powder up to concentrations of 0.05% (500 ppm), 0.07%, and 0.10%. The mixtures were extruded at 250°C and were transformed into 0.25-mm-thick films. These films were used as the starting material in the LTHA and in the DSC measurements. Aging was carried out in ovens at 140°C. This experiment provided OIP data (in days).

DSC measurements were carried out in the temperature range from 150 to 350°C, where an exothermic peak due to polymer oxidation is observed. Five different heating rates were used: 2, 5, 10, 15, and 20 K/min. OIT was calculated using the Fitter program [63] as described in [56].

The results of all experiments are schematized in Fig. 1. The X data are OIT values obtained by DSC. They form a three-way block [62]: 25 antioxidant samples \times 3 antioxidant concentrations \times 5 heating rates. The Y data are OIP values obtained by LTHA. They form a two-way block (matrix): 25 antioxidant samples \times 3 antioxidant concentrations.

The Fitter program was employed in nonlinear regression analysis [61]. The Unscrambler program was used [72] in PLS modeling. SIC was performed using software made as an Add-In for the Excel package. The NIPALS algorithm [5] was used in the SIC method for bilinear modeling. The standard SIMPLEX algorithm [65] was used in optimization. All necessary procedures were used in data preprocessing, transformations, etc. Now this program is in beta testing.

SOFT MODELING

The data set was processed using the soft approach that combined the PLS method [5, 21] for calibration and the SIC method [35] for constructing prediction intervals.

Initially, the three-way X data were unfolded into a flat matrix (25 \times 15) as shown in Fig. 2. It is important that the error in OIP is not constant and grows with increasing OIP value. This can be due to two circumstances. The first is the above-mentioned visual inspec-

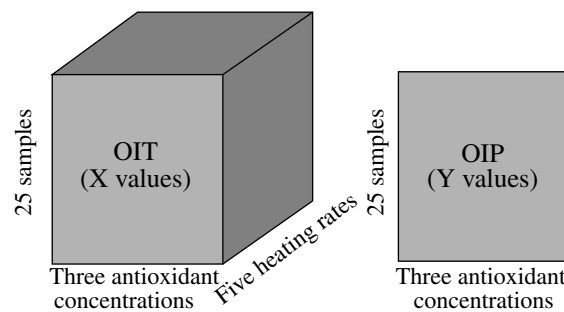


Fig. 1. Graphical representation of data (see explanation in text).

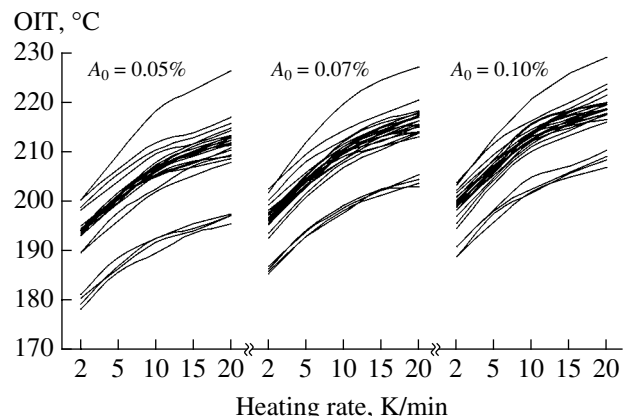


Fig. 2. Schematic presentation of X-data for PLS modeling: relationship between OIT and the heating rate for various initial antioxidant concentrations.

tion method, whose accuracy is lower for more stable (that is long-lived) antioxidants. The second is that, in our sample preparation procedure, a small amount of antioxidant is mixed with a large amount of PP. This leads inevitably to some heterogeneity in the antioxidant distribution in PP. In order to compensate for the inconstancy of the OIP measurement error, we used the square root transformation of all OIP values. Furthermore, we centered X and Y data in PLS modeling.

In the construction of the linear calibrating model

$$y = \mathbf{X}\mathbf{a} + \mathbf{\epsilon}, \quad (1)$$

the main mathematical difficulty is to invert the matrix $\mathbf{X}^T \mathbf{X}$, which, in our case, has dimensions of 15 \times 15. If this matrix were nondegenerate (full-rank), such calibration could be performed using the ordinary least-squares procedure to estimate the unknown model parameters: $\hat{\mathbf{a}} = (\mathbf{X}^T \mathbf{X})^{-1} \mathbf{X}^T \mathbf{y}$. However, in our case, the matrix is degenerate, as in most practical problems. As was mentioned above, this obstacle is circumvented by using various methods of regularization, for example, principal component analysis and ridge regression. We chose the PLS method [5]. Its essence is the simulta-

Table 1. Main properties of the PLS models constructed for various initial antioxidant concentrations

$A_0, \%$	$X_{\text{expl}}, \%$	$Y_{\text{expl}}, \%$	RMSEC	r_{cal}^2	r_{test}^2	β
0.05	99	92	0.287	0.96	0.99	0.84
0.07	99	88	0.342	0.93	0.99	1.02
0.10	99	84	0.395	0.91	0.97	1.20

neous decomposition of the matrix \mathbf{X} and vector \mathbf{y} and their representation in the form of

$$\mathbf{X} = \mathbf{TP}^t + \mathbf{E}, \quad \mathbf{y} = \mathbf{Tq} + \mathbf{f}, \quad (2)$$

where \mathbf{T} is the score matrix, \mathbf{P} and \mathbf{q} are the loading matrix and vector, and \mathbf{E} and \mathbf{f} are the residual matrix and vector. In this decomposition, three circumstances are taken into consideration. First, the columns t_i of the matrix \mathbf{T} are linear combinations of the columns x of the matrix \mathbf{X} ; that is $t_i = \mathbf{Xw}_i$. Second, the coefficients w are chosen in such a way as to maximize the correlation between the response \mathbf{y} and t_i . Third, the number of columns in the matrices \mathbf{T} and \mathbf{P} must be equal to the effective rank of the matrix \mathbf{X} . This value (r) is called the number of PLS components, and it is obviously smaller than the number of columns in \mathbf{X} . As a result of this decomposition, the initial calibration problem (1) is projected onto a subspace of a smaller dimension, where the new problem (2) is nondegenerate. An important advantage of the PLS method is that it allows data to be visualized as the score plots (in the PLS component coordinates PC1–PC2). We will make use of this advantage. The PLS method is described in numerous publications (see, for example, references in [5, 20]), which are, however, hardly available in Russia. Recently, a correct but brief description of this method has appeared in a textbook [63]. A detailed description of the PLS method and other multivariate data analysis methods in Russian can be found in [6].

Applying the PLS method to our example, we divided the overall data set into two parts. The calibration set includes 18 samples (AO-1 through AO-18). These data were employed to construct the model. The second, test set consists of seven samples (AO-19 through AO-25). These data were employed in model validation. For each initial antioxidant concentration A_0 , its own PLS model with two PLS components was built. The main features of these models are presented in Table 1. In this table, for each initial antioxidant concentration, the following values characterizing the quality of the model are presented. The explained variances of \mathbf{X} and \mathbf{y} are the averaged residuals calculated with the calibration set ($\mathbf{X}_{\text{cal}}, \mathbf{y}_{\text{cal}}$) of model (2):

$$X_{\text{expl}} = 1 - \frac{\|\mathbf{X}_{\text{cal}} - \mathbf{TP}^t\|^2}{\|\mathbf{X}_{\text{cal}}\|^2},$$

$$Y_{\text{expl}} = 1 - \frac{\|\mathbf{y}_{\text{cal}} - \mathbf{Tq}\|^2}{\|\mathbf{y}_{\text{cal}}\|^2}.$$

They characterize the accuracy with which the data are approximated (explained) by the PLS method. Root-mean-square errors are derived from the calibration data set as

$$\text{RMSEC} = \frac{\|\mathbf{y}_{\text{cal}} - \mathbf{Tq}\|}{\sqrt{n_{\text{cal}} - r}}. \quad (3)$$

They characterize the accuracy of response modeling. In the above formulas, n_{cal} is the number of data in the calibration set and r is the number of PLS components. The norm of a matrix (vector) is the square root of the sum of the squares of its components. The correlation coefficients for the measured and predicted values for the calibration (r_{cal}^2) and test (r_{test}^2) sets are calculated in a usual way. The last column of Table 1 is the SIC calibration error (β), which is explained below.

Using the PLS method, we obtain the average point estimate of OIP. In order to find the interval prediction, we employed the SIC method. This method is based on the only assumption that all errors involved in the multivariate calibration are bounded. Under this assumption, there is a positive β value such that

$$\text{Prob}\{|\varepsilon| > \beta\} = 0 \quad (4)$$

and for any $0 < b < \beta$ $\text{Prob}\{|\varepsilon| > b\} > 0$,

where Prob is probability of the event. The value of β is called the maximum error deviation. It characterizes the calibration error and can be estimated by conventional statistical methods [46]. The β values obtained for the data examined are presented in Table 1.

Based on postulate (4) and using the given calibration set $\{\mathbf{X}, \mathbf{y}\}$ with n samples, one can construct a set of inequalities regarding the unknown regression parameters \mathbf{a} . This set will define a closed convex set in the space of parameters:

$$A = \{\mathbf{a} \in \mathbb{R}^p : \mathbf{y}^- < \mathbf{Xa} < \mathbf{y}^+\}. \quad (5)$$

Here, $y_j^- = y_j - \beta$, $y_j^+ = y_j + \beta$, $j = 1, \dots, n$. The set A is the region of possible values. It is a volumetric analogue of the ordinary point estimate $\hat{\mathbf{a}}$ obtained by conventional regression methods (for example, PLS). Using the set A , one can predict the response y for any given (new) vector \mathbf{x} . Obviously, if the parameter \mathbf{a} changes within A , then the corresponding predicted value $\hat{y} = \mathbf{x}^t \mathbf{a}$ will remain inside the interval

$$V = [v^-, v^+], \quad (6)$$

where

$$v^- = \min_{\mathbf{a} \in A} (\mathbf{x}^t \mathbf{a}), \quad v^+ = \max_{\mathbf{a} \in A} (\mathbf{x}^t \mathbf{a}).$$

These equations represent a typical problem of linear programming [64]. The optimum of a linear form $\mathbf{x}^t \mathbf{a}$ is known to be achieved in one of the vertices of the convex set A . A standard numerical procedure (Simplex algorithm) allows one to move from one vertex to another in the direction of the maximum change (increase or decrease) of the form, and this makes it possible to carry out optimization in such a way that it is unnecessary to construct a set A explicitly. However, a bounded solution of the linear programming problem exists if and only if the set A is bounded. It is well known [65, 66] that A is bounded if and only if \mathbf{X} is a full-rank matrix. Therefore, in the rank deficiency case, which is a typical of practical problems, one should use some regularizing procedure, for example, PLS. Subsequently, the regular score matrix \mathbf{T} (2) should be used in place of the initial matrix \mathbf{X} (1) in the SIC method.

The results of PLS/SIC prediction for the initial antioxidant concentration $A_0 = 0.05\%$ are shown in Fig. 3. Here, the predicted OIP values are plotted against the corresponding measured values, the square root being taken of both of them. Each sample (the points A are calibration samples, and the points B are test samples) is shown together with two error intervals. The horizontal bars are error intervals for the measured OIP values, and they are equal to the doubled value of the maximum error deviation β for all samples. The vertical bars indicate the prediction intervals (6), and they vary from one sample to another. Obviously, for all calibration samples, the prediction interval is always less than or equal to the error interval. This is the fundamental feature following immediately from SIC theory.

HARD MODELING

Hard models for OIP prediction are constructed for each particular type of antioxidant. To do this, 25 horizontal “cuts” are chosen in the overall data set shown in Fig. 1. This leads to 25 sets of data, specifically, matrices \mathbf{X}_i with dimensions 5×3 and vectors \mathbf{y}_i of length 3.

The calibration procedure for these data consists of two steps. In the first step, a model describing antioxi-

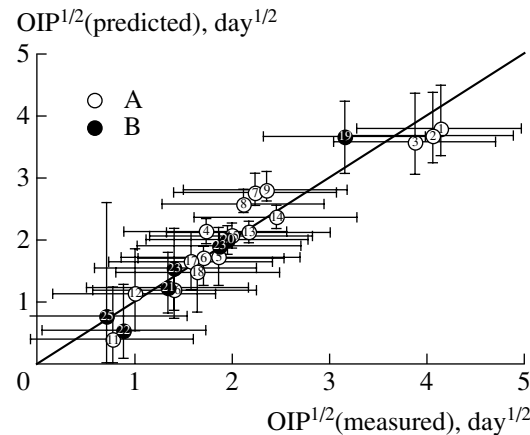


Fig. 3. Prediction of the induction period using the soft approach for an initial antioxidant concentration of 0.05%. Relation between the square roots from predicted and measured values. A—calibration samples; B—test samples. The horizontal bars show β values (calibration error), and the vertical bars indicate SIC (prediction) intervals.

dant consumption during a DSC run is constructed. This is X data calibration. The regression model is an implicit function relating OIP, the initial antioxidant concentration A_0 , and the heating rate v . This function depends nonlinearly on the unknown kinetic parameters to be estimated by nonlinear regression (NLR) analysis. In the second step of calibration, a model describing antioxidant consumption during LTHA is constructed. This is Y data calibration. This regression model explicitly expresses OIP as a function of the exposure temperature (T_e) and the initial antioxidant concentration. This function involves the same kinetic parameters as the first model. Their estimates are found in the first step, while in the second step, a special error propagation procedure is employed to estimate the uncertainty in the predicted induction period.

Let us consider the first step of calibration. Antioxidant is consumed in the course of material aging. The OIP value is defined by the point in time at which the antioxidant is spent up to some critical value A_c , which is temperature-dependent according to the Arrhenius law [55]:

$$A_c = k_c \exp\left(-\frac{E_c}{RT}\right). \quad (7)$$

During oxidation, antioxidant is consumed according to the law

$$\frac{dA}{dt} = -kA, \quad (8)$$

$$A(0) = A_0,$$

where A is the current antioxidant concentration and k is the reaction rate constant, which depends on temperature according to the Arrhenius law

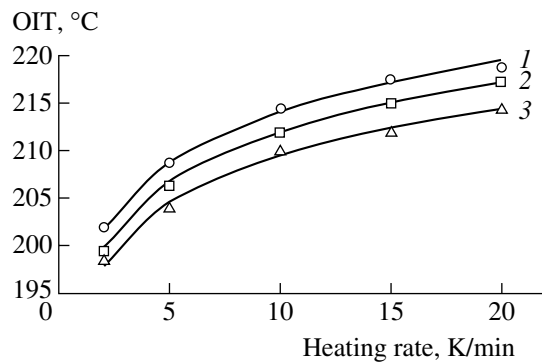


Fig. 4. Relation between the oxidation initial temperature of PP in the system PP + AO-1 and the heating rate for various initial antioxidant concentrations, %: (1) 0.1, (2) 0.07, and (3) 0.05. The points are experimental data, and the curves represent calibration data.

$$k = k_a \exp\left(-\frac{E_a}{RT}\right).$$

In the DSC runs, a sample is heated at the rate v from the initial temperature $T_0 = 293$ K:

$$T(t) = T_0 + vt.$$

In this case, a solution of Eq. (8) can be presented as

$$A(t) = A_0 \exp(-k_a Z(t)), \quad (9)$$

where the function $Z(t)$ is

$$Z(t) = \int_0^t \exp\left(-\frac{E_a}{R(T_0 + vs)}\right) ds.$$

This integral can be expressed in terms of the standard integral exponential function $E_n(z)$ [67],

$$E_n(z) = \int_1^\infty t^{-n} e^{-zt} dt \quad (n = 0, 1, 2, \dots; z > 0).$$

It is convenient to represent Z as a function of temperature T rather than time t :

$$Z(T) = \frac{1}{v} \left[T E_2\left(\frac{E_a}{RT}\right) - T_0 E_2\left(\frac{E_a}{RT_0}\right) \right]. \quad (10)$$

Inserting Eq. (10) into Eq. (9) and setting the current antioxidant concentration to be equal to the critical concentration A_c from Eq. (7), we obtain the equation

$$A_0 \exp(-k_a Z(T)) = k_c \exp\left(-\frac{E_c}{RT}\right), \quad (11)$$

which implicitly defines the dependence of the OIT T on the unknown parameters and known experimental conditions. However, it is inconvenient to utilize this

equation in practice. Let us set it in a form more appropriate for parameter estimation. After taking the logarithm and making some simplifications, one obtains

$$\exp(a) E_2\left(\frac{E_a}{RT}\right) T + v \left(c - a - \frac{E_c}{RT} \right) = 0, \quad (12)$$

where $a = \ln k_a$ and $c = \ln k_c$.

In this equation, temperature T is the response, and the heating rate v and the initial concentration A_0 are predictors (experimental factors). The variables a , E_a , c , and E_c are the unknown parameters that are estimated from experimental data. When seeking the estimates, one has to repeatedly solve Eq. (12) for T ,

$$T = T(v, A_0; a, E_a, c, E_c), \quad (13)$$

for each given set of predictors v and A_0 , and to find such values (estimates) of a , E_a , c , and E_c that minimize the sum of squares

$$\min_{a, E_a, c, E_c} \sum_{ij} [Y_{ij} - T(v_j, A_{0i}; a, E_a, c, E_c)]^2. \quad (14)$$

Here, Y_{ij} are the measured OIT values, the index i stands for three initial antioxidant concentrations, and the index j numerates five heating rates v .

In the minimization of sum (14), we face significant difficulties. First of all, function (13) cannot be represented explicitly and even cannot be expressed implicitly in terms of elementary functions. Secondly, it is obvious that the function given by Eq. (12) depends nonlinearly on the unknown parameters. Finally, sum (14) minimization is a stiff problem [3, 67]. All of these circumstances make the model calibration a complicated computational problem. This problem was solved with the use of the Fitter program [61], which is appropriate for solving such problems. This software implements a stable gradient minimization approach based on the matrix exponent technique [68]. This approach has shown high efficiency exceeding the efficiency of the popular Levenberg-Marquardt approach [69, 70] in the solution of stiff problems. Besides, the regression equations in the Fitter program may be defined in a natural algebraic form admitting implicit expressions. Finally, a very important feature of the software is that the derivatives are calculated automatically by symbolic differentiation, ensuring high calculation accuracy.

The first model calibration for AO-1 is illustrated in Fig. 4. Experimental data (points) and the corresponding calibration curves are shown.

Let us consider the second step of modeling, in which the model of antioxidant consumption during LTHA is constructed. The solution of Eq. (8) for constant conditions ($T = \text{const}$) appears as

$$A(t) = A_0 \exp(-kt).$$

In order to find the induction period t_i (OIP), the current concentration $A(t)$ should be set equal to the critical concentration A_c defined by Eq. (7). Thus,

$$t_i = \left[\frac{E_c}{RT_e} + \ln A_0 - c \right] \exp \left(\frac{E_a}{RT_e} - a \right), \quad (15)$$

where T_e is the aging temperature. In our case, $T_e = 140^\circ\text{C}$ or 413 K.

The estimates of the parameters $\hat{\boldsymbol{\theta}} = (\hat{a}, \hat{E}_a, \hat{c}, \hat{E}_c)$ found in the first step of calibration should be employed in Eq. (15). In order to find a point estimate for the induction period and to determine the confidence interval, the uncertainty in these estimates should be taken into consideration. Unfortunately, the conventional error propagation method [17]

$$\text{var}(f) = \frac{\partial f(\hat{\boldsymbol{\theta}})}{\partial \boldsymbol{\theta}} \text{cov}(\hat{\boldsymbol{\theta}}, \hat{\boldsymbol{\theta}}) \frac{\partial f(\hat{\boldsymbol{\theta}})}{\partial \boldsymbol{\theta}}$$

cannot be applied to Eq. (15) because of the nonlinearity of the model. An accurate confidence interval can be obtained by a statistical simulation or, more precisely, by using the free simulation approach [23]. In this method, the confidence interval for the function $f(\boldsymbol{\theta})$ is calculated as the percentile of a sampling $\{f(\boldsymbol{\theta}_1), f(\boldsymbol{\theta}_2), \dots\}$, in which the $f(\boldsymbol{\theta}_i)$ values are calculated in the simulation of parameters $\boldsymbol{\theta}_i$ in accordance with the normal distribution $N(\hat{\boldsymbol{\theta}}, \text{cov}(\hat{\boldsymbol{\theta}}, \hat{\boldsymbol{\theta}}))$.

An example of confidence prediction constructed by means of this approach for AO-18 is shown in Fig. 5. The confidence probability here is $P = 0.90$. The confidence intervals for the other samples are presented in Fig. 6.

It is important that, in hard modeling (NLR), we did not use the OIP values obtained in long-term aging. Therefore, these values may be employed in the model validation by calculating the root-mean-square error of prediction (RMSEP),

$$\text{RMSEP} = \frac{\|\mathbf{y}_{\text{test}} - \mathbf{Tq}\|}{\sqrt{n_{\text{test}} - r}},$$

which is shown in Table 2. At the same time, the root-mean-square error of calibration (RMSEC) (3), which is a conventional measure of accuracy, cannot be estimated because not the OIP, but the OIT values were calibrated as a function of v and A_0 in the first step of modeling. However, the residual sum of squares can be found for each antioxidant and the standard deviation for OIP estimates can be calculated (entry 4 in Table 2).

COMPARISON OF METHODS

Let us compare the results of hard (NLR) and soft (PLS/SIC) modeling obtained for a common data set.

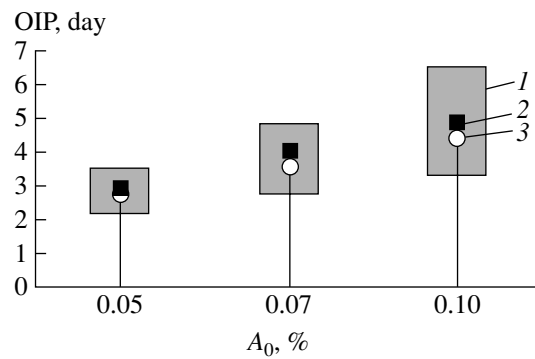


Fig. 5. Prediction of the induction period (OIP) in the system PP + AO-18 for various initial antioxidant concentrations: (1) confidence intervals for $P = 0.90$, (2) point estimates, and (3) measured values.

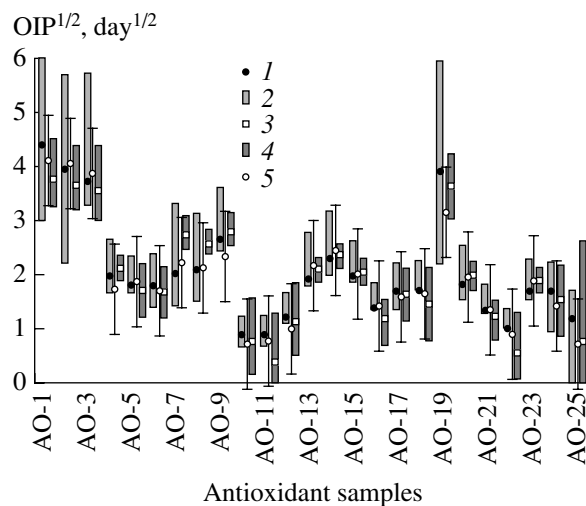


Fig. 6. Results of OIP prediction for various antioxidant samples with an initial concentration of 0.05%: (1, 2) hard (NLR) prediction, (3, 4) soft (PLS/SIC) modeling, (5) measured values with vertical bars indicating the measurement (calibration) error in β . Square root is taken from all values.

These models utilize data in different ways. There are 25 hard models constructed for each particular antioxidant and three soft models constructed for each initial antioxidant concentration.

Figure 6 summarizes the results obtained by both approaches for the initial concentration 0.05%. The results of hard modeling (NLR) (points 1 and rectangles 2 of confidence intervals for a probability of 0.90) and of the soft method (PLS/SIC) (points 3 and rectangles 4 of prediction intervals) are plotted here. The reference OIP values measured in LTHA are represented by points 5, with error intervals equal to the maximum error deviation β . In order to make the comparison clearer, the square root was taken from all OIP values. Such plots can also be constructed for the data subsets corresponding to the initial antioxidant concentrations 0.07 and 0.10%. They appear similar.

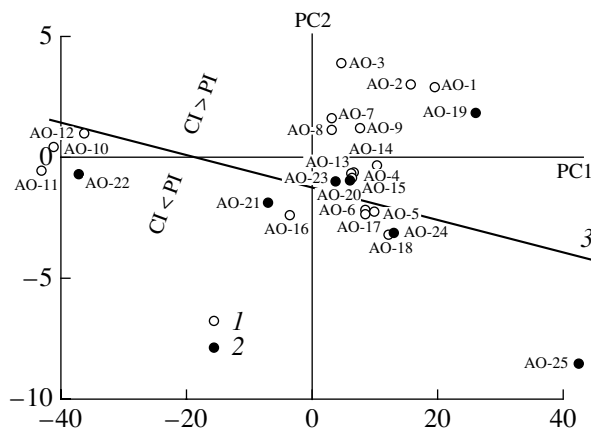


Fig. 7. PLS score plot for samples with $A_0 = 0.05\%$: (1) calibration samples and (2) test samples. Line 3 separates the samples for which the confidence interval (CI) is narrower (wider) than the prediction interval (PI).

Some general statistical features of the hard (NLR) and soft (PLS/SIC) approaches are presented in Table 2. The following designations are used here for the measured and predicted X (OIT) and Y (OIP) values. \mathbf{X} and $\hat{\mathbf{X}}$ are the measured and predicted OIT values, $\mathbf{y} = \sqrt{\mathbf{IP}}$ is the square root of the measured OIP value, $\hat{\mathbf{y}}_i$ is the corresponding vector obtained by taking the square root from the OIP estimates obtained by the hard (NLR, $i = 1$) and soft (PLS/SIC, $i = 2$) methods, and w_i is equal to the width of the confidence (NLR, $i = 1$) and prediction (PLS/SIC, $i = 2$) intervals. The square root was taken from all intervals. For brevity, confidence and prediction intervals will be designated CI and PI, respectively. The former were obtained by hard modeling; the latter, by the PLS/SIC soft approach.

Examination of Table 2 and Fig. 6 suggests the following inferences. The approaches provide similar accuracies (entry 1 in Table 2) and biases (entry 2). The

accuracy decreases as the initial antioxidant concentration is increased. The PLS/SIC method affords better results for lower initial antioxidant concentrations, whereas NLR is better for higher concentrations. However, on the average, the point estimates are similar (entry 3). X (OIT) values are well modeled with both approaches, but the hard approach (NLR) does this a little bit better (entry 4).

The interval estimates are also very close on the average (entry 5), although CIs can differ greatly from PIs for some samples (see entry 6 in Table 2 and Fig. 6). The CI width increases with an increase in OIP for all initial antioxidant concentrations, whereas the PI width does not depend on y (entry 7 in Table 2). This indicates that the response transformation $y = \sqrt{OIP}$ does produce the expected effect in PLS/SIC modeling, but cannot improve the results of NLR modeling.

As can be seen from Table 2 (entry 5), the width of the prediction intervals increases with an increase in the initial antioxidant concentration. This is even more evident from the hard model (15), which establishes a relationship between the induction period t and A_0 . This can by no means be foreseen within the soft PLS-modelling. Apparently, this fact is a consequence of a fundamental property of the polymer system. Specifically, the greater the amount of antioxidant added, the less accurate the prediction of the induction period. From this standpoint, the hard and soft approaches produce similar results. At the same time, the results of these approaches can be quite different for some samples. As can be seen from Fig. 6, for some samples (for example, AO-5, AO-6, AO-10, and AO-11), CI is narrower than PI, whereas for other samples (for example, AO-1, AO-2, and AO-3), the reverse is true. It would be interesting to understand why CI and PI values differ so greatly.

Figure 7 shows PLS scores (that is, the X data projection onto the subspace of two principal PLS components—PC1 and PC2) for samples with the initial anti-

Table 2. Statistical characteristics of the prediction obtained by the hard (NLR) and soft (PLS/SIC) methods

No.	Statistical features of prediction	NLR ($i = 1$, CI)			PLS/SIC ($i = 2$, PI)		
		Initial antioxidant concentration, %					
		0.05	0.07	0.10	0.05	0.07	0.10
1	RMSEP, day ^{1/2}	0.242	0.246	0.272	0.239	0.251	0.336
2	Bias, day ^{1/2}	0.087	0.058	0.040	0.011	0.004	0.002
3	Correlation ($\hat{\mathbf{y}}_1$, $\hat{\mathbf{y}}_2$)	0.953	0.934	0.916	0.953	0.934	0.916
4	Average value ($\mathbf{X} - \hat{\mathbf{X}}$) ² , K ²	—	0.224	—	0.286	0.286	0.286
5	Average value (w_i)	1.038	1.151	1.397	0.934	1.204	1.476
6	Correlation (w_1 , w_2)	0.202	0.007	0.028	0.202	0.007	0.028
7	Correlation (y , w_i)	0.815	0.846	0.836	-0.184	-0.161	-0.113

oxidant concentration of 0.05%. (AO-1, ..., AO-18 are calibration samples, and AO-19, ..., AO-25 are test samples). Clearly, AO-25 is an obvious outlier (or, more precisely, outsider in SIC theory, which will be considered below). The value predicted for AO-25 differs only slightly from the measured value; however, this sample is far from the center of the PLS model. This is the reason why the prediction uncertainty for AO-25 is high, and this sample has the widest SIC interval (Fig. 6), being a unique test sample for which the prediction error is greater than the calibration error. It can be seen in Fig. 7 that all samples for which the confidence interval (CI by NLR) is narrower than the prediction interval (PI by SIC) are in the left lower part of the plot, below straight line 3. This line separates the totality of samples into two parts, specifically, samples for which $CI > PI$ and for which $CI < PI$.

This result seems to be surprising. We expected to observe some patterns in interval widths (i.e., prediction accuracies) for the samples examined. In fact, there is a structure classifying the samples according to the method (hard or soft) that is more appropriate for them. It would be interesting to examine the plot resulting from the hard NLR method and to see if similar structures are there. The correlation between the E_c and \hat{c} estimates is shown in Fig. 8 (see Eq. (12)). Note that there is a significant correlation between the estimated parameters in the pairs (a , E_a) and (c , E_c). In the Arrhenius equation, the correlation between the preexponential factor and the activation energy is often close to unity [71]. In our case, $\text{cor}(\hat{a}, \hat{E}_a) = 0.995$ and $\text{cor}(\hat{c}, \hat{E}_c) = 0.997$. Figure 8 enables us to look at the problem from another angle. It clearly shows that all samples for which the hard (NLR) approach is better ($CI < PI$) are on the lower part of the plot, under line 4. Transition is observed at a critical antioxidant concentration of 0.016% at $T = 140^\circ\text{C}$.

The score plot in Fig. 7 represents only one subset of samples, namely, samples with the initial antioxidant concentration of 0.05%. The plots for $A_0 = 0.07\%$ and $A_0 = 0.10\%$ have the same structure and are not presented here. However, the parameter estimates (c , E_c) were obtained by the hard modeling, in which all samples with various initial antioxidant concentrations were processed together by NLR. Therefore, Fig. 8 presents the overall data set. This circumstance suggests a conclusion that is important in selecting a calibration approach. Whether CI from NLR is wider or narrower than PI from SIC does not depend on the initial antioxidant concentration, but does depend on the critical antioxidant concentration, which is a property of the antioxidant itself. Thus, NLR will always be better (worse) than PLS/SIC for a given antioxidant, irrespective of the initial antioxidant concentration. The hard approach will be precise for the antioxidants with a low critical concentration, while the soft method

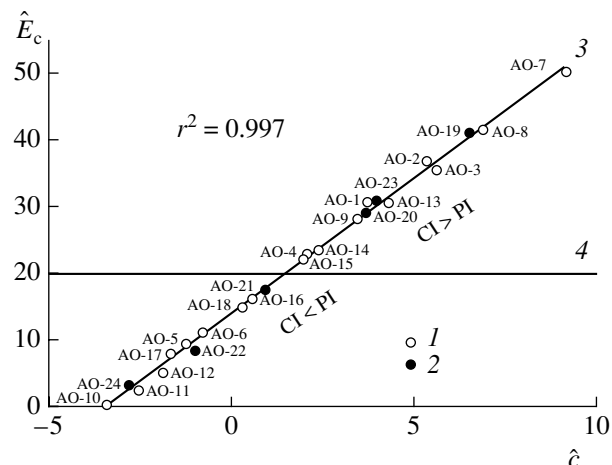


Fig. 8. Correlation between the estimates of the preexponential factor (\hat{c}) and the corresponding activation energy (\hat{E}_c): (1) calibration samples and (2) test samples. Line 3 shows the correlation trend. Line 4 separates the samples for which $CI > PI$.

PLS/SIC will be precise for the antioxidants with a high value of A_c .

Another important aspect that should be considered when comparing modeling methods is the limitations imposed on their domains of applicability. Hard modeling (NLR) offers an obvious advantage here, because it can be used in the prediction of the induction period at various antioxidant concentrations and at various exposure temperatures. The prediction of the induction period for AO-18 at an initial concentration of 0.04% and an exposure temperature in the range $80^\circ\text{C} < T < 200^\circ\text{C}$ is illustrated in Fig. 9. Obviously, these conditions were not examined experimentally. The results presented were obtained by extrapolating Eq. (15) to these conditions. The soft method cannot provide such a prediction. The data obtained for $T = 200^\circ\text{C}$ are very important, because polypropylene is processed at this temperature. On the other hand, the application of the hard nonlinear model to conditions lying far from the experimental area is rather risky. In particular, this model cannot be used in the extrapolation to room temperature. Therefore, the service life of polypropylene cannot be predicted from DSC data. In other words, we cannot precisely bound the region in which the hard method is applicable.

The situation with the PLS/SIC soft method is quite different. Here, the applicability range can be determined exactly. Figure 10 shows the test samples in the SIC object status plot (OSP), which is used to establish applicability limits. SIC classification theory is detailed in [35, 45, 46]. Here, we present a very brief description of this method. Each sample from the test set (AO-18, ..., AO-25) is represented on the OSP in the following coordinates. The SIC residual is the difference between the center of the prediction interval (6) and the corresponding reference value divided by the maximum

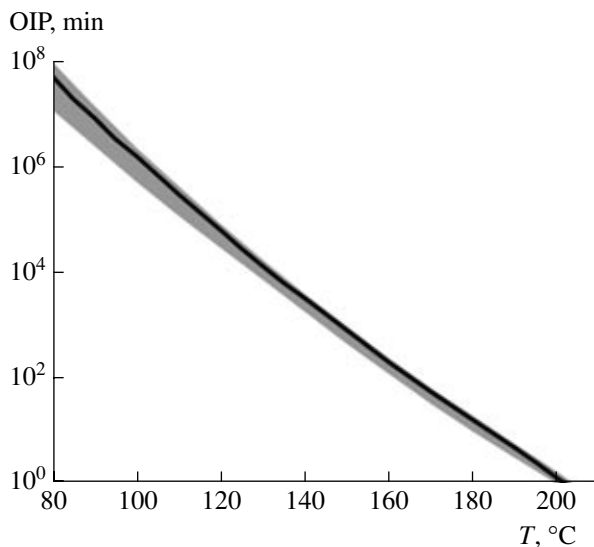


Fig. 9. Prediction of the induction period (OIP) depending on the exposure temperature for AO-18 with an initial concentration of 0.04%. The line indicates the average value, and the gray corridor shows the confidence interval for $P = 0.95$.

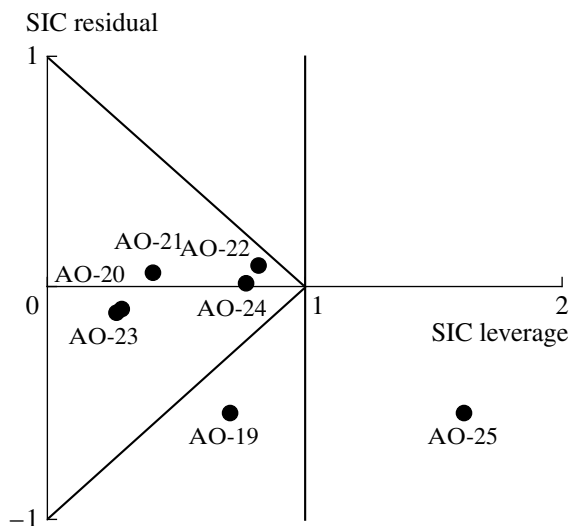


Fig. 10. SIC object status plot for test set with $A_0 = 0.07\%$.

error deviation β defined by Eq. (4). The SIC leverage is equal to the half-width of the prediction interval divided by β . The position of a test (or new) sample on this plot determines the possibility of constructing a prediction for this sample. All samples situated inside the triangle (AO-20, AO-21, ..., AO-24) are called insiders. They are in full agreement with the model, and the prediction for them is the most reliable. Samples lying beyond the model are called outsiders (AO-19 and AO-25). The outsiders are not in conflict with the model, but the prediction for them is less accurate. This is explained either by a large leverage (AO-25) or by a large bias (AO-19). Thus, utilizing the SIC object status

technique, one can classify a new sample and bound the applicability range of the PLS/SIC method.

Note that the applicability ranges of the hard and soft methods are quite different in nature. In the hard approach, the applicability range is the range in the factor space (T and A_0) to which the model may be extrapolated. Here, we deal with the same antioxidant, which was preliminarily investigated by DSC. In the soft approach the applicability range is the range of new antioxidants to which the constructed PLS/SIC model may be applied. Here, the experimental conditions (that is, the initial antioxidant concentration and the heating rate in DSC) must be the same as for the calibration set utilized. One more circumstance is relevant to this consideration. Let us assume that model improvement and a higher accuracy are desired. In the hard method, a model is constructed for each particular antioxidant. Therefore, new experiments with other initial concentrations of the same antioxidant should be carried out. This will increase the prediction accuracy for this antioxidant, and there will be no influence on the prediction quality for the other antioxidants.

CONCLUSIONS

We have demonstrated that, in the antioxidant activity problem, long-term and expensive thermal aging can be replaced with fast DSC measurements followed by data processing using a hard (NLR) or soft (PLS/SIC) method. Both approaches to calibration predict the induction period with a satisfactory degree of accuracy that is not worse than the error in the conventional approach. Therefore, both methods can be recommended for practice.

Each calibration approach has its own advantages and disadvantages. The hard approach enables one to obtain predictions extrapolated to conditions (temperature and concentration) lying beyond the range of the experiment. However, such extrapolation cannot be constrained; therefore, the result is sometimes unreliable. On the other hand, the soft approach has a rigorously defined applicability that can be bounded by means of the SIC object status approach. At the same time, the PLS/SIC method cannot be employed in the prediction of the induction period under conditions differing from those in the calibration experiment. Both approaches have the same prediction accuracy and show similar behaviors towards prediction conditions: the greater the initial antioxidant concentration, the worse the accuracy of prediction. However the hard approach gives better results for the antioxidants with a low critical concentration (that is, for the antioxidants with a short induction period), whereas the soft approach is better in the opposite case. This is the fundamental, inherent property of an antioxidant that is independent of the initial antioxidant concentration.

Thus, in the case when the prediction of the behavior of a given polymer system is the goal of the investi-

gation, the hard approach is preferable. In the case when the investigator wishes to compare the activities of various antioxidants, the soft model is better.

The hard approach establishes a relationship between experimental factors and responses, taking into account the notion of chemical and physical processes occurring in the system. This leads to rather complicated mathematical models requiring special computational methods for their processing. However, if these models adequately describe the process examined, they allow extrapolation, or, in other words, a prediction going beyond the experimental range of factors.

The soft approach does not require deep knowledge of the nature of the investigated phenomenon. The mathematical models utilized in this approach are linear in the unknown parameters and are, therefore, simple in use and interpretation. However, for constructing such models, it is often required to guess an appropriate factor or response transformation leading to system linearization. In the example of antioxidant activity prediction considered here, the square root was successfully taken from all experimental values of the induction period and the desired result was thereby achieved. Therefore, the soft approach requires that the researcher have some experience in solving similar problems. At the same time, this approach produces reliable results in very different areas. It works well in solving classification problems or interpolation (that is, in prediction for (nearly) the same conditions as in the experiment). It is impossible to apply this approach to extrapolation problems.

REFERENCES

1. Lavrent'ev, M.M., Kraeva, A.G., and Bukhgeim, A.V., *Obratnaya zadacha khimicheskoi kinetiki* (Inverse Problem of Chemical Kinetics), Novosibirsk: Vychislitel'nyi Tsentr Sib. Otd. Akad. Nauk SSSR, 1980.
2. Spivak, S.I. and Gorskii, V.G., *Dokl. Akad. Nauk SSSR*, 1981, vol. 257, no. 2, p. 412.
3. *Primenenie vychislitel'noi matematiki v khimicheskoi fizicheskoi kinetike* (Computational Mathematical Methods in Chemical and Physical Kinetics), Polak, L.S., Ed., Moscow: Nauka, 1969.
4. Pavlov, B.V. and Brin, E.F., *Khim. Fiz.*, 1984, vol. 3, no. 3, p. 393.
5. Esbensen, K.H., *Multivariate Data Analysis in Practice*, CAMO, 2000.
6. Esbensen, K., *Analiz mnogomernykh dannykh* (Multivariate Data Analysis), Rodionova, O., Ed., Barnaul: Altaisk. Gos. Univ., 2003.
7. Haario, H. and Taavitsainen, V.-M., *Chemom. Intell. Lab. Syst.*, 1998, vol. 44, p. 77.
8. Bijlsma, S., Louwerse, D.J., Windig, W., and Smilde, A.K., *Anal. Chim. Acta*, 1998, vol. 376, p. 339.
9. Bijlsma, S., Louwerse, D.J., and Smilde, A.K., *J. Chemom.*, 1999, vol. 13, p. 311.
10. Taavitsainen, V.-M. and Haario, H., *J. Chemom.*, 2001, vol. 15, p. 215.
11. De Juan, A., Maeder, M., Martinez, M., and Tauler, R., *Chemom. Intell. Lab. Syst.*, 2000, vol. 54, p. 123.
12. De Juan, A., Maeder, M., Martinez, M., and Tauler, R., *Anal. Chim. Acta*, 2001, vol. 442, p. 337.
13. Bezemer, E. and Rutan, S.C., *Chemom. Intell. Lab. Syst.*, 2001, vol. 59, p. 19.
14. Brin, E.F. and Pomerantsev, A.L., *Khim. Fiz.*, 1986, vol. 5, no. 12, p. 1674.
15. Pomerantsev, A.L. and Rodionova, O.Ye., *Chemom. Intell. Lab. Syst.*, 1999, vol. 48, p. 121.
16. Rodionova, O.E. and Pomerantsev, A.L., *Usp. Khim.* 2006, vol. 75, p. 302.
17. Bard, Y., *Nonlinear Parameter Estimation*, New York: Academic, 1974.
18. Pirson, K., *Philos. Mag.*, 1901, vol. 2, no. 6, p. 559.
19. Demidenko, E.Z., *Lineinaya i nelineinaya regressii* (Linear and Nonlinear Regressions), Moscow: Finansy i Statistika, 1981.
20. Tikhonov, A.N., *Dokl. Akad. Nauk SSSR*, 1963, vol. 4, p. 1035.
21. Höskuldsson, A., *Prediction Methods in Science and Technology*, Copenhagen: Thor, 1996.
22. Faber, K., *Chemom. Intell. Lab. Syst.*, 2000, vol. 52, p. 123.
23. Pomerantsev, A.L., *Chemom. Intell. Lab. Syst.*, 1999, vol. 49, p. 41.
24. Kantorovich, L.V., *Sib. Mat. Zh.*, 1962, vol. 3, no. 5, p. 701.
25. Voshchinin, A.P., Bochkov, A.F., and Sotirov, G.R., *Zavod. Lab.*, 1990, vol. 56, no. 7, p. 76.
26. Anisimov, V.M., Pomerantsev, A.L., Novoradovskii, A.G., and Karpukhin, O.N., *Zh. Prikl. Spektrosk.*, 1987, vol. 46, p. 117.
27. Akhunov, I.R., Akhmadishin, Z.Sh., and Spivak, S.I., *Khim. Fiz.*, 1982, vol. 12, p. 1660.
28. Bakhitova, R.Kh. and Spivak, S.I., *Izv. Vyssh. Uchebn. Zaved., Khim. Khim. Tekhnol.*, 1999, vol. 42, p. 92.
29. Slin'ko, M.G., Spivak, S.I., and Timoshenko, V.I., *Kinet. Katal.*, 1972, vol. 13, p. 1570.
30. Spivak, S.I., Timoshenko, V.I., and Slin'ko, M.G., *Dokl. Akad. Nauk SSSR*, 1970, vol. 192, p. 580.
31. Belov, V.M., Karbainov, Yu.A., Sukhanov, V.A., et al., *Zh. Anal. Khim.*, 1994, vol. 49, p. 370.
32. Khlebnikov, A.I., *Zh. Anal. Khim.*, 1996, vol. 51, p. 347.
33. Belov, V.M., Sukhanov, V.A., and Unger, F.G., *Teoreticheskie i prikladnye aspekty metoda tsentra neopredelennosti* (Theoretical and Applied Aspects of the Uncertainty Center Method), Novosibirsk: Nauka, 1995.
34. Pomerantsev, A.L. and Rodionova, O.Ye., *Chemom. Intell. Lab. Syst.*, 2005, vol. 79, nos. 1–2, p. 73.
35. Rodionova, O.Ye., Esbensen, K.H., and Pomerantsev, A.L., *J. Chemom.*, 2004, vol. 18, p. 402.
36. Westad, F. and Martens, H., *J. Near Infrared Spectrosc.*, 2000, vol. 8, p. 117.
37. Cook, R.D., *Technometrics*, 1977, vol. 19, p. 15.
38. Cook, R.D., *J. Am. Stat. Ass.*, 1979, vol. 74, p. 169.
39. Andrews, D.F. and Pregibon, D., *J. R. Stat. Soc. B*, 1978, vol. 40, p. 84.

40. Draper, N.R. and John, J.A., *Technometrics*, 1981, vol. 23, p. 21.
41. Næs, T., *J. Chemom.*, 1989, vol. 1, p. 121.
42. Höskuldsson, A., *Chemom. Intell. Lab. Syst.*, 2001, vol. 55, p. 23.
43. Jouan-Rimbaud, D., Massart, D.L., Saby, C.A., and Puel, C., *Anal. Chim. Acta*, 1997, vol. 350, p. 149.
44. Fernandez Pierna, J.A., Wahl, F., de Noord, O.E., and Massart, D.L., *Chemom. Intell. Lab. Syst.*, 2002, vol. 63, p. 27.
45. Pomerantsev, A.L. and Rodionova, O.E., *Zh. Anal. Khim.*, 2006, no. 10 (in press).
46. Rodionova, O.Ye. and Pomerantsev, A.L., in *Progress in Chemometrics Research*, Pomerantsev, A.L., Ed., New York: Nova Science, 2005, p. 43.
47. Pomerantsev, A.L. and Rodionova, O.Ye., in *Progress in Chemometrics Research*, Pomerantsev, A.L., Ed., New York: Nova Science, 2005, p. 209.
48. Pomerantsev, A.L. and Rodionova, O.Ye., in *Aging of Polymers, Polymer Blends and Polymer Composites*, Zaikov, G.E., Ed., New York: Nova Science, 2002, vol. 2, p. 19.
49. Pomerantsev, A., Rodionova, O., and Höskuldsson, A., *Chemom. Intell. Lab. Syst.*, 2006, vol. 81, p. 165.
50. Clancey, V.J., *Nature*, 1947, vol. 159, p. 339.
51. Rajkó, R., *Anal. Lett.*, 1994, vol. 27, p. 215.
52. Eriksson, L., Johansson, E., Kettaneh-Wold, N., and Wold, S., *Multi- and Megavariate Data Analysis*, Umeå: Umetrics, 2001.
53. Burden, F.R., Rosewarne, B.S., and Winkler, D., *Chemom. Intell. Lab. Syst.*, 1997, vol. 38, p. 127.
54. Héberger, K. and Borosy, A.P., *J. Chemom.*, 1999, vol. 13, p. 473.
55. Slyapnikov, Yu. A., in *Developments in Polymer Stabilization*, London: Applied Science, 1981, vol. 5.
56. Bystritskaya, E.V., Pomerantsev, A.L., and Rodionova, O.Ye., *J. Chemom.*, 2000, vol. 14, p. 667.
57. Maksimova, G.A. and Pomerantsev, A.L., *Zavod. Lab.*, 1995, vol. 61, p. 432.
58. Pomerantsev, A.L., *Chemom. Intell. Lab. Syst.*, 2003, vol. 66, p. 127.
59. Bystritskaya, E.V., Pomerantsev, A.L., and Rodionova, O.Ye., *Conferentia Chemometrica (CC-97)*, Budapest, 1997; <http://sol.cc.u-szeged.hu/~rajko/Pos54.gif>.
60. Bystritskaya, E.V., Pomerantsev, A.L., and Rodionova, O.Ye., *Proc. 5th Scandinavian Symp. on Chemometrics (SSC5)*, Lahti, 1997, p. 46.
61. Fitter Add-In [On line], <http://polycert.chph.ras.ru/fitter.htm> (October 1, 2006).
62. Smilde, A., Bro, R., and Geladi, P., *Multi-Way Analysis with Application in the Chemistry Sciences*, New York: Wiley, 2004.
63. Kellner, R.A., Mermet, J.-M., and Otto, M., *Analytical Chemistry*, Weinheim: Wiley-VCH, 2001.
64. Taha, H., *Operations Research: An Introduction*, New York: Macmillan, 1982.
65. Gass, S., *Linear Programming*, New York: McGraw-Hill, 1975.
66. Kuhn, H.W. and Tucker, A.W., *Linear Inequalities and Related Systems*, Annals of Mathematics Studies, Princeton: Princeton Univ. Press, 1956, vol. 38.
67. Abramowitz, M. and Stegun, I.A., *Handbook of Mathematical Functions*, New York: National Bureau of Standards, 1964.
68. Pavlov, B.V. and Povzner, A.Ya., *Zh. Vychisl. Mat. Mat. Fiz.*, 1973, vol. 13, p. 1056.
69. Marquardt, D.W., *SIAM J.*, 1963, vol. 11, p. 431.
70. Levenberg, K., *Q. Appl. Math.*, 1944, vol. 2, p. 164.
71. Rodionova, O.E. and Pomerantsev, A.L., *Kinet. Katal.*, 2005, vol. 46, no. 3, p. 329 [*Kinet. Catal.* (Engl. Transl.), vol. 46, no. 3, p. 305].
72. Unscrambler [On line], <http://www.camo.no> (October 1, 2006).